NASA/TM-20205005815

Status of Analysis and Manufacturability of Superconducting Wires With Low AC Losses

Gerald V. Brown and Jeffrey J. Trudell
Glenn Research Center, Cleveland, Ohio

Lee W. Kohlman
Ames Research Center, Moffett Field, California

Kirsten P. Duffy
The University of Toledo, Toledo, Ohio

F. David Koci
Vantage Partners, LLC, Brook Park, Ohio

October 2020

NASA STI Program . . . in Profile

Since its founding, NASA has been dedicated to the advancement of aeronautics and space science. The NASA Scientific and Technical Information (STI) Program plays a key part in helping NASA maintain this important role.

The NASA STI Program operates under the auspices of the Agency Chief Information Officer. It collects, organizes, provides for archiving, and disseminates NASA's STI. The NASA STI Program provides access to the NASA Technical Report Server—Registered (NTRS Reg) and NASA Technical Report Server—Public (NTRS) thus providing one of the largest collections of aeronautical and space science STI in the world. Results are published in both non-NASA channels and by NASA in the NASA STI Report Series, which includes the following report types:

- TECHNICAL PUBLICATION. Reports of completed research or a major significant phase of research that present the results of NASA programs and include extensive data or theoretical analysis. Includes compilations of significant scientific and technical data and information deemed to be of continuing reference value. NASA counter-part of peer-reviewed formal professional papers, but has less stringent limitations on manuscript length and extent of graphic presentations.

- TECHNICAL MEMORANDUM. Scientific and technical findings that are preliminary or of specialized interest, e.g., "quick-release" reports, working papers, and bibliographies that contain minimal annotation. Does not contain extensive analysis.

- CONTRACTOR REPORT. Scientific and technical findings by NASA-sponsored contractors and grantees.

- CONFERENCE PUBLICATION. Collected papers from scientific and technical conferences, symposia, seminars, or other meetings sponsored or co-sponsored by NASA.

- SPECIAL PUBLICATION. Scientific, technical, or historical information from NASA programs, projects, and missions, often concerned with subjects having substantial public interest.

- TECHNICAL TRANSLATION. English-language translations of foreign scientific and technical material pertinent to NASA's mission.

For more information about the NASA STI program, see the following:

- Access the NASA STI program home page at http://www.sti.nasa.gov

- E-mail your question to help@sti.nasa.gov

- Fax your question to the NASA STI Information Desk at 757-864-6500

- Telephone the NASA STI Information Desk at 757-864-9658

- Write to:
  NASA STI Program
  Mail Stop 148
  NASA Langley Research Center
  Hampton, VA 23681-2199

NASA/TM-20205005815

Status of Analysis and Manufacturability of Superconducting Wires With Low AC Losses

Gerald V. Brown and Jeffrey J. Trudell
Glenn Research Center, Cleveland, Ohio

Lee W. Kohlman
Ames Research Center, Moffett Field, California

Kirsten P. Duffy
The University of Toledo, Toledo, Ohio

F. David Koci
Vantage Partners, LLC, Brook Park, Ohio

National Aeronautics and
Space Administration

Glenn Research Center
Cleveland, Ohio 44135

October 2020

This work was sponsored by the Advanced Air Vehicle Program
at the NASA Glenn Research Center

Level of Review: This material has been technically reviewed by technical management.

Available from

NASA STI Program
Mail Stop 148
NASA Langley Research Center
Hampton, VA 23681-2199

National Technical Information Service
5285 Port Royal Road
Springfield, VA 22161
703-605-6000

This report is available in electronic form at http://www.sti.nasa.gov/ and http://ntrs.nasa.gov/

Contents

Status of Analysis and Manufacturability of Superconducting Wires With Low AC Losses

Gerald V. Brown and Jeffrey J. Trudell
National Aeronautics and Space Administration
Glenn Research Center
Cleveland, Ohio 44135

Lee W. Kohlman
National Aeronautics and Space Administration
Ames Research Center
Moffett Field, California 94035

Kirsten P. Duffy
The University of Toledo
Toledo, Ohio 43606

F. David Koci
Vantage Partners, LLC
Brook Park, Ohio 44142

Summary

Superconductors can carry an order-of-magnitude higher current than room temperature copper wires and can do so with two orders-of-magnitude lower alternating current (AC) electrical losses. These advantages underlie our estimates that turboelectric propulsion of large aircraft can be enabled by superconducting machines. However, even the much smaller losses of superconductors pose thermal management issues at the low temperatures required for superconductivity, and predicting those losses and validating the predictions has been a developing process at NASA Glenn Research Center over the last decade.

Since Glenn's earliest assessments of the feasibility of fully superconducting machines for turboelectric propulsion, the available models of AC losses in superconductors have changed significantly, as well as the state of development of superconducting wire for the coils of electric machines. While the models available to us have improved significantly, the value of the AC losses predicted by these models have only increased as more fidelity was developed. The fabrication of medium temperature superconducting wires ($T_c \approx 40$ K) has advanced, and wires can be produced with finer filaments and tighter twisting than a decade ago. However, the ideal wire configurations, developed decades ago for low-temperature superconductors ($T_c < 25$ K), still elude manufacturers of medium- and high-temperature ($T_c > 77$ K) superconductors. This report discusses the developments, the current limitations, and the expectations that future configurations of superconducting wire can yet be produced that will provide suitably low AC losses for the aircraft propulsion application.

The report presents a basic discussion of the types of AC losses in superconductors, followed by a discussion of the evolution of our understanding of the practical consequences of those AC losses. Next, there is a discussion of the superconducting wire configurations that have been developed, which were partially guided by that understanding. A brief discussion of the modes of removing the heat produced by

the losses is presented. Lastly, a comparison is presented between losses in currently available MgB_2 wire and other important cases, including copper at room temperature, copper at liquid hydrogen temperature, and expected future MgB_2 wire. Room temperature copper has 100 times the loss of today's MgB_2 and 300 times the expected loss of future MgB_2. That implies we can expect much higher efficiency from fully superconducting machines than from machines with copper stators, and high-efficiency targets remain the driver behind investment in MgB_2 development and medium-temperature superconductor research.

Introduction

Since the beginning of our assessment of turboelectric propulsion of transport aircraft, it has been clear that fully superconducting electric machines are best suited to meet, simultaneously, the required efficiency and low weight for large, long-range aircraft. Fully superconducting machines are those with superconducting wire in both rotating and stationary parts of the machine (also known as rotor and stator). The assessment of fully superconducting machines in turboelectric, distributed propulsion aircraft has been discussed previously (Felder, Kim, and Brown, 2009) and (Brown, 2011). Superconducting machines can fundamentally achieve both higher electrical efficiency and high specific power (or power density) than conventional machines. The N3X aircraft assessments predicted a nominally 20-percent fuel burn improvement for the superconducting, fully distributed architecture over an equivalent vehicle with advanced turbofan engines mounted on pylons. The aircraft power-distribution system provides additional constraints that guide the superconducting electric machine development. High operating frequencies in the range of 200 to 400 Hz are required because of the desired shaft speeds of the turbine engines and of the propulsive fans. High-voltage distribution in the range of 1 to 10 kV is required to keep the electric currents to manageable magnitudes. Superconducting distribution throughout the aircraft is required to avoid the efficiency losses and weight penalties associated with stepping back and forth between cryogenic and noncryogenic components.

Superconductors offer no electrical resistance to the flow of steady unidirectional current when operated suitably below their critical temperatures, currents, and magnetic fields. However, in nonsteady conditions, such as alternating current (AC) and alternating electromagnetic fields, a superconductor coil is resistive due to several loss mechanisms that actually have analogues in nonsuperconducting electromagnetic applications. The rotor windings of electric machines operate with application of direct current (DC). Superconducting technology in DC applications is comparatively mature and will not be discussed at length here. Stator windings, however, carry AC and are subject to alternating magnetic fields created by both the rotor and stator. Configurations of superconducting wires have been developed that can reduce AC losses to an acceptable level for the standard electric grid frequencies of 50 and 60 Hz (Meyerhoff, 1995), and superconducting components for terrestrial power grids are beginning to appear. Nevertheless, as noted previously, the frequencies required for turboelectric aircraft propulsion are several times higher, and since one type of superconductor AC loss increases with the square of frequency, that loss is higher by more than an order of magnitude.

The favorite superconductors for most applications would be the high-temperature superconductors (HTSs), which maintain superconductivity at the highest temperatures. The HTS materials are brittle compounds that are commercially available in thin, wide composite tapes. It is the large width of the tape superconductor that makes HTS unsuitable for this application, because the large width results in large AC losses that are exacerbated at the relatively high AC frequencies needed for turboelectric propulsion. Low- and medium-temperature superconducting wires are both available in round cross sections and thus are better candidates for high-frequency AC applications. The low-temperature superconductor NbTi is a

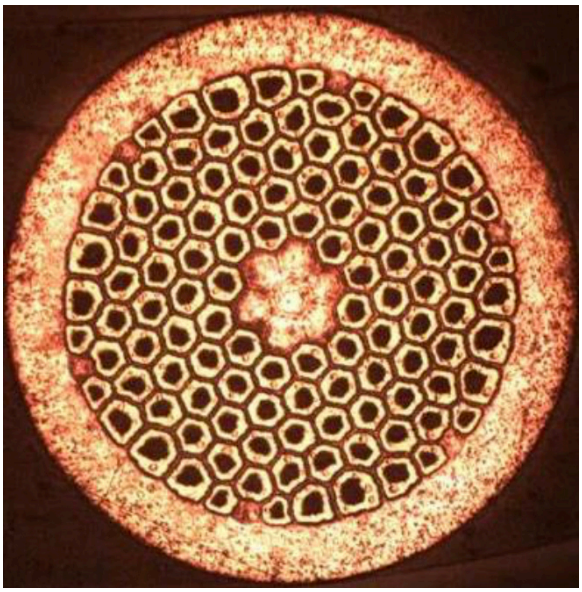

Figure 1.—MgB_2 composite conductor with 78 superconducting filaments (roughly circular black areas). Around each filament is lighter colored tube of pure Nb that protects superconductor from diffusion of impurities during heat treat. All other materials are various Cu-Ni alloys.

ductile metallic alloy with a critical temperature of only 9.2 K and can be made in suitable composite wire forms, but has a higher cooling requirement burden. MgB_2, which has a critical temperature of 39 K and can be made in a round-wire, multifilament composite form such as is shown in Figure 1 (from Tomsic et al., 2015), is the most mature medium-temperature superconductor and is the focus of this report. The available multifilament MgB_2 conductors have superconductor filaments surrounded by a supporting matrix of several materials that serve manufacturing and structural functions.

This report discusses the maturity of MgB_2 fabrication and the modeling of electrical losses in MgB_2 coils relevant for megawatt- (MW-) class electric machines. Although the engineering task of estimating how much loss can be practically removed from the superconductor is largely deferred to a subsequent report, some possible modes and magnitudes of heat removal are presented. Relevant supporting calculations and relationships about losses in electric machine stators are derived in appendixes.

Types of AC Losses in Superconductors

The following reviews the electrical loss mechanisms that must be understood and considered in designing low loss electric machines. Many of these same considerations apply to nonsuperconducting electric machines, but are described here in terms of application to superconducting wires and coils. It should be remembered that nonsuperconducting wires also incur AC losses and their resistive losses occur even for DC.

Hysteresis Loss

When a magnetic field is applied by an external source to a solid superconducting wire or to a single filament of a multifilamentary conductor, the penetration of that field into the superconductor is opposed by the superconductor in a manner that dissipates energy. Energy is dissipated as well during the

reduction of the field. The process is somewhat analogous to the hysteresis loss in a magnetic material. For each filament in a multifilamentary wire, the average power P_h dissipated over time in an AC situation is proportional to the product of the filament diameter d_f, the electrical frequency f_e, and the amplitude B of the applied field:

$$P_h = \left(\frac{8}{3\pi}\right) J_c B\, d_f\, f_e\, V_{\text{filaments}} \tag{1}$$

where J_c is the critical current density in the superconducting filaments and $V_{\text{filaments}}$ is the volume of the superconducting filaments only. The wire geometrical property that can reduce this loss is the filament diameter d_f. Thus, we desire a conductor with a large number of very small filaments. It is shown in Appendix A that the ratio of hysteresis loss to the shaft power P_{shaft} of a superconducting machine is

$$\frac{P_h}{P_{\text{shaft}}} = \left(\frac{32}{3\pi}\right)\left(\frac{f_e}{f_s}\right)\left(\frac{d_f}{r}\right)\left(\frac{J_c}{J}\right) \tag{2}$$

where f_s is the shaft frequency of revolution, r is the average radius of the stator, and J is the amplitude of the operating current density in the superconducting filaments.

For typical superconducting machine values of $(f_e/f_s) = 3$, $(J_c/J) = 2$, and $r = 0.2$ m, and for an assumed filament diameter of 10 μm, the hysteresis loss as a fraction of machine total power would be 0.001 or 0.1 percent, which if this were the only loss, would give a machine efficiency of 99.9 percent. This was the original reason for high hopes of high efficiency from the fully superconducting machine and we have used 10 μm as our goal for filament diameter for some time.

As a guide to what may be possible in the future, it may be noted that some of the low-temperature superconductors have been developed with extremely fine filaments. Niobium tin, Nb_3Sn, a brittle intermetallic superconductor that can be synthesized in a manner similar to one of the methods of making MgB_2, has been produced in a composite conductor with 7-μm-diameter filaments. The ductile superconducting alloy NbTi has been produced in wire form with filaments of submicron diameter (Carr and Wagner, 1986). This might be indicative of what could be produced in the future for MgB_2.

Rotating Field Hysteresis Loss

A rotating field of constant amplitude produces a different loss than does a purely oscillatory field. Combinations of rotating and oscillating fields actually are the rule in an electric machine stator. The combination of the field of the rotor and the field of the stator leads to total field vectors that trace out a variety of shapes that can be nearly linear, nearly elliptical, or rather irregular. Some examples of calculated fields in a concentrated, rectangular stator coil are shown in Figure 2. It is surprising that, although the part of the field due to the stator alone appears very elliptical, when the rather dog-bone-shaped field of the rotor is added, the sum is closer to oscillatory than to rotational.

Lorin and Masson (2013) have developed a model for losses in combined oscillatory and rotational magnetic fields, but that model has not yet been incorporated into our models of the electrical machines. That report presents the distributions of current density over the cross section of a single superconducting filament for various elliptical fields. For purely rotating fields that are sufficiently larger than those necessary for full penetration into the superconducting filament, Carr (2001, p. 101) indicates that the loss for a purely rotating field is π/2 times the loss for a purely oscillating field. For this limit of a purely rotating field, the Lorin and Masson model and Carr are in agreement. However, results for lower strength

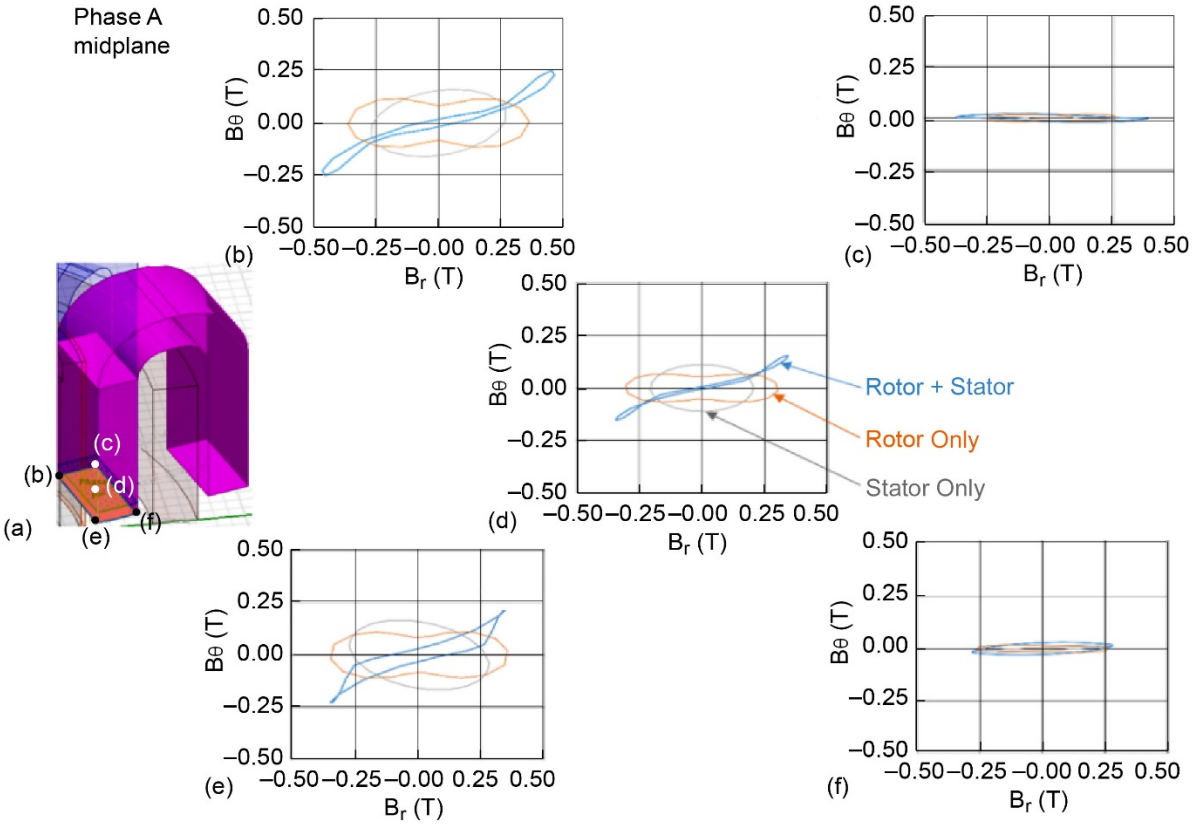

Figure 2.—Field in stator is not a simple combination of oscillating and rotating fields. Field varies in form depending on position in stator. (a) Stator. Position on stator (b) upper left, (c) upper right, (d) center, (e) lower left, and (f) lower right.

elliptical fields, other than those of Lorin and Masson, are not available. As a conservative approach to estimating the hysteresis loss, we are incorporating the high-field correction into our loss models as new calculations are performed. Equation (1) is henceforth to be replaced by the following hysteresis loss, which is larger by the factor of π/2:

$$P_h = \left(\frac{4}{3}\right) J_c B d_s V_{\text{filaments}} \tag{3}$$

Eddy Current and Coupling Losses

There are two named losses in superconducting wires due to currents induced by externally varying magnetic fields. One, explicitly called the eddy current loss, arises from closed loops of current that flow longitudinally in the normal metal matrix down one side of a wire, cross over to the other side of the wire to flow back longitudinally in the matrix and then cross back to the first side to close the circuit. The longitudinal parts of this loop are wholly in the normal resistive material, and energy is dissipated along all parts of the circuit. Similarly, the “coupling loss” arises from closed loops of current. However, in this second case, the longitudinal parts of the path are in the superconducting filaments rather than in the normally conducting matrix. The crossover portions of the loop for both eddy current and coupling losses are through normally conducting matrix material. The coupling loss is usually much larger than the eddy current loss since the longitudinal superconducting paths support stronger currents. The resistance of the

eddy current circuit is higher, and somewhat counterintuitively, yields a lower loss. It is helpful to realize that the familiar expression for power loss in a resistor, $P = I^2 R$ can be rewritten, by noting that $V = I \cdot R$, as $P = V^2 / R$. The driving voltage V is fixed by the area enclosed by the eddy current path. Then a lower path resistance R is seen to result in higher AC loss. The eddy current loss is typically negligible in cases of interest to us and we do not consider it further herein.

As explained, the coupling loss arises because an externally applied field induces currents that flow down one superconducting filament for some distance, crosses through the various matrix materials in the wire to another superconducting filament, flows back through that filament to near the starting point, and crosses back through the various materials to the original filament to complete a circuit. The loss is reduced if the distance between the crossover points is smaller. Twisting the wire forces the crossover areas to occur at a distance of half of the twist pitch apart.

The time-averaged value P_c of the coupling loss (from Carr 2001, Equation (9.5), p. 127) is

$$P_c = \left(\frac{1}{2\rho_{eff}} \right) \left(B L_t f_e \right)^2 V_{\text{matrix}} \tag{4}$$

where L_t is the twist pitch of the filaments, ρ_{eff} is an effective transverse resistivity of the metals in the crossover regions, and V_{matrix} is the volume of the nonsuperconducting part of the composite. It is seen that this loss depends quadratically on field amplitude, twist pitch, and electrical frequency. Particularly troublesome for us is the quadratic dependence on frequency because aerospace power applications require relatively fast machines compared to most industrial machines. The required frequencies may be as high as 400 Hz, as compared to the conventional power line frequency of 60 Hz. This high frequency arises from a desired high shaft speed of the power turbine in a turboshaft engine. A shaft speed of 8,000 rpm in a generator with three pole pairs would yield an electrical frequency of $(8{,}000/60) \cdot 3 = 400$ Hz. The wire parameters that can reduce the coupling loss are the twist pitch, which should be minimized, and the effective resistivity of the matrix, which should be maximized. Unfortunately, an appropriate value of effective resistivity is not easy to estimate, since it typically involves several different materials and a complicated geometry. One can hope only to approximate its value. Reducing the twist pitch is very beneficial because it reduces the area available to intercept the change in flux that generates the electromotive force that drives the loop current that generates the coupling loss. The quadratic dependence on pitch can be inferred from the fact that ohmic loss in a circuit can be written as V^2 / R (an alternative form to the familiar $I^2 R$) and by noting that the V generated is proportional to the projected area of one-half of a twist pitch. The resistance of the loop (which is relatively independent of the twist pitch) comes solely from the normal resistance where the coupling current must travel through the matrix material as it crosses between filaments.

It is sometimes useful to know the ratio of the coupling loss to the hysteresis loss. Appendix B derives that ratio.

Prior to 2014, the coupling loss equation we were using was not Equation (4). Previously, we erroneously used a formula in our electric machine loss calculations that accounted for only half the loss values. The corrected value shown in Equation (4) is now used in all of our machine models.

Transport Current Loss

The transport current loss is essentially a hysteresis loss due to the magnetic field caused by the current flowing in a filament rather than by an externally applied magnetic field. It depends on the filament critical current as well as the ratio of the AC amplitude to the filament critical current, which is the operating fraction. Let the operating fraction be denoted by $\gamma \equiv I_o/I_c$ where I_o is the amplitude of the AC in the filament and I_c is the critical current of the filament, then the transport current loss P_ℓ in the filament per unit length of filament (from Carr 2001, Equation (7.88), p. 102) is

$$P_\ell = \frac{\mu_o}{\pi} f_e I_c^2 \left[\frac{(1-\gamma)\ln(1-\gamma) + \gamma - \gamma^2}{2} \right] \tag{5}$$

where f_e is the frequency of the transport current and μ_o is the permeability of free space.

The dependence of the value of the term in the square brackets on the operating ratio γ is shown in Figure 3. It is clear from the figure that the transport loss can be reduced by operating the superconductor well below its critical current. For example, at an operating current I_o of 50 percent of I_c, the factor in the square brackets of Equation (5) is 0.0284. On a volume basis for a multifilament superconducting wire with a superconductor volume fraction of λ and a filament diameter d, the transport current loss P_t is

$$P_t = \frac{\mu_o}{4} f_e d^2 J_c^2 \left[\frac{(1-\gamma)\ln(1-\gamma) + \gamma - \gamma^2}{2} \right] V_{\text{filaments}} \tag{6}$$

In terms of the volume of an entire wire V_{wire}:

$$P_t = \frac{\mu_o}{4} f_e d^2 J_c^2 \lambda \left[\frac{(1-\gamma)\ln(1-\gamma) + \gamma - \gamma^2}{2} \right] V_{\text{wire}} \tag{7}$$

This loss is typically smaller than other losses unless there are magnetic components in the matrix material of the composite conductor.

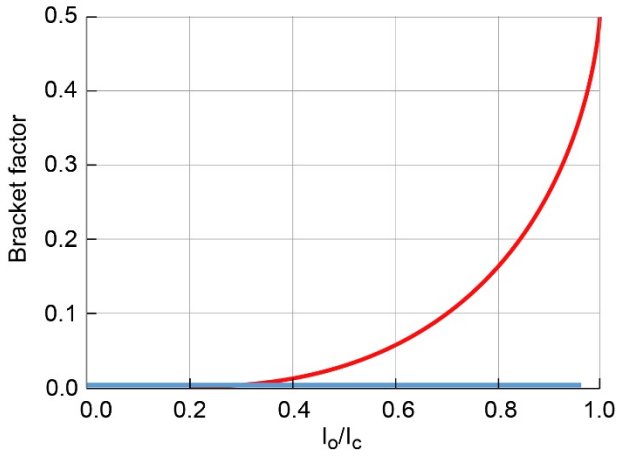

Figure 3.—Bracket factor in Equation (7).

Evolution of Models of Superconductor AC Loss at NASA Glenn Research Center

There was a considerable period of development of our models of superconducting loss at NASA Glenn Research Center. This gradual development occurred as our contractors gained understanding of the new requirements imposed by the high operating frequency of the superconductors in aircraft power train motors and generators.

Hysteresis Only

The original superconducting AC loss estimate at Glenn was developed under contract and included only the hysteresis AC loss. Previously studied systems were typically at lower frequencies, and hysteresis loss was expected to be the dominant loss. Furthermore, the smallest MgB_2 superconducting filaments at the time were on the order of 70 μm in diameter, which would indeed drive a large hysteresis loss and render the coupling loss negligible in comparison. But our sights were necessarily set on developing finer filaments, so our contractor supplied models for coupling and eddy current losses.

For a set of standard conditions of magnetic field $B = 0.5$ T, temperature $T = 25$ K, electrical frequency $f_e = 200$ Hz, filament diameter = 70 μm, and superconducting fraction of 12 percent, the hysteresis loss per unit volume of superconducting strand (i.e., based on the whole wire volume, not just the filament volume) was predicted to be 1.75 W/cm^3 using Equation (1). If the filament size were reduced to 10 μm, the hysteresis loss would drop to 0.25 W/cm^3. This was "state-of-the-art" in our superconducting loss predictions when a 1-MW machine demonstration was proposed in 2010.

It is briefly argued in a subsequent section on Heat Removal Capability that it is feasible to extract up to 2 or 3 W/cm^3 of AC loss from a MgB_2 superconducting wire by a stream of either liquid hydrogen or gaseous helium in direct contact with the wire and flowing parallel to the wire. It is further argued that epoxy-impregnated coils can also be cooled if the number of layers is small. Hence, our original estimates of superconductor AC loss did not cause us concern about the feasibility of cooling, at either the global energy balance level, or at the local level due to limits imposed by heat transfer to a coolant, even for 70-μm-diameter filaments. However, that original estimate based only on oscillating hysteresis loss was unfortunately only a part of the story. The remainder of this section about the evolution of models deals with other aspects that were considered, especially the inclusion of the coupling loss.

"Kim" Improvement on Hysteresis Loss Model

The hysteresis loss models, shown as Equations (1) and (3), are based on the so-called Bean model (Bean, 1962) that describes how magnetic flux penetrates into a superconducting material. Note the presence of the factor J_c. The J_c changes with B, decreasing as B increases. Nevertheless, the Bean approximation uses a single value of J_c, which is based on the amplitude of the externally applied magnetic field, even though the strength of that field varies as $B\sin(\omega t)$ and is therefore weaker throughout most of the cycle period and the field internal to the filament varies with position and time as well. Thus, J_c is higher on average, giving an average loss greater than that predicted by Equation (4). Taking proper account of the B and J_c changes over a cycle was the improvement over the Bean model suggested by Kim (Kim, Hempstead, and Strnad, 1963). We do not use this enhancement because suitable analysis is not available.

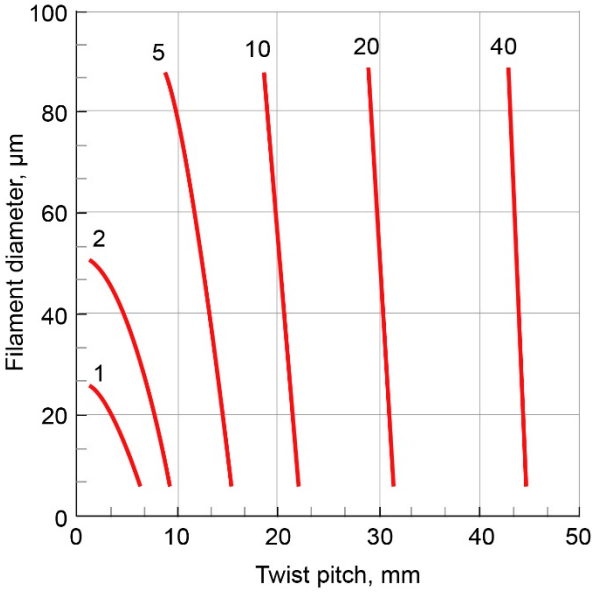

Figure 4.—Contour plot of AC losses (watts per unit volume of wire) as functions of filament size and twist pitch for one particular value of matrix effective resistivity at 25 K and 0.5 T field amplitude for wide range of filament size and twist pitch.

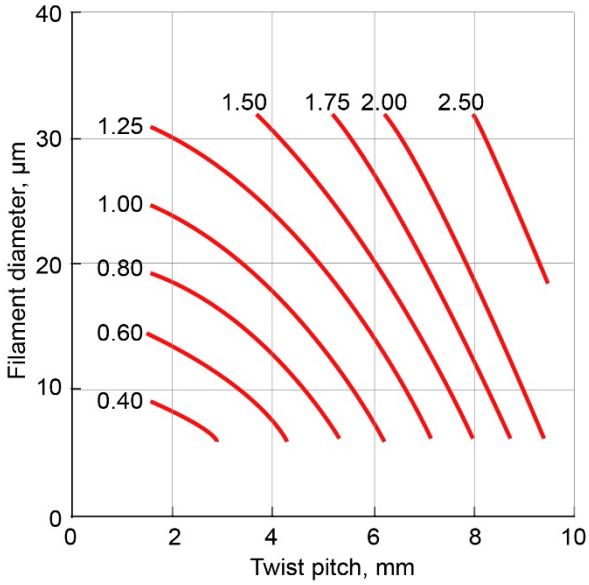

Figure 5.—Contour plot of AC losses (watts per unit volume of wire) as functions of filament size and twist pitch for one particular value of matrix effective resistivity at 25 K and 0.5 T field amplitude for range of filament size and twist pitch more relevant for application in electric machine stators.

Hysteresis and Corrected Coupling Loss Combined

All of our recent analyses have used the combination of hysteresis loss, augmented to allow for purely rotating fields, and the corrected coupling loss. A contour plot of the sum of the hysteresis and coupling losses is shown in Figure 4, as a function of filament diameter and twist pitch, for an assumed effective transverse resistivity ρ_{eff} of 13.8 μΩ·cm. Transverse resistivity assumptions will be discussed in detail in the later sections of this report dealing with wire development. It can be seen for the standard set of conditions (B = 0.5 T, T = 25 K, and f_e = 200 Hz), a filament diameter of 70 μm, and a superconducting fraction of 12 percent, that the loss per wire volume is over 10 W/cm^3 of wire for a twist pitch of 20 mm or more. Such a high level of loss appears to be intractable for the intended aeronautics application. That is why fabrication trials that demonstrate coils wound with wire with finer filaments and tight twist pitch were a necessary tollgate prior to further machine development. A narrower range of filament size and twist pitch is shown in Figure 5. As will be noted later, filament size as small as 10 μm and twist pitch as small as 5 mm have been achieved (though not simultaneously). Volumetric losses below 2 W/cm^3 appear possible with the assumed value of transverse resistivity.

Transport Current Loss Inclusion

The transport current loss introduced previously and formulated in Equations (5) to (7) was said to be small. Let us consider some actual numbers. For wire produced by the domestic manufacturer Hyper Tech Research, Inc., the superconductor fraction λ is typically ~12 to 15 percent for a single-restack wire and ~7 to 10 percent for a double-restack wire. For a superconductor fraction of 12 percent, f_e of 200 Hz, T of 25 K, B of 0.5 T, and operating current fraction of 0.5, the transport current loss is only 0.0012 W/cm^3 of wire, which is negligible compared to the hysteresis and coupling losses.

It has been shown experimentally with short samples that a magnetic matrix material in the superconducting strand can increase the transport loss by a factor as large as 10 or even 100 (Sumption et al., 2016). In short sample segments, the induced magnetic flux lines are circular. The reluctance along the flux lines that lie within the wire will be reduced if the matrix is magnetic, and hence the strength of the magnetic field will be increased, which in turn increases the loss. However, when a superconducting wire is part of a coil, or if there is an external source of magnetic field such as a rotor, the magnetic field lines do not form a closed circuit within that wire. The magnetic material may well constitute only a minor portion of an entire magnetic circuit and the presence of magnetic material in the superconducting composite wire therefore may reduce the reluctance by a negligible amount. It can thereby be argued that the transport loss will not be important in a superconducting coil. However, experimental verification is required to judge the relative importance of this loss contribution confidently.

Summary of AC Loss Model Changes

Focused modeling of AC losses for superconducting electric machines relevant to aeronautics applications began with estimation of hysteresis loss in 2007. The hysteresis loss estimate has since been increased by about 60 percent to cover the possibility of rotating fields, for a given set of conductor and field parameters. Although the estimated loss value attributed to hysteresis has increased for any specific parameter set, a reduction of filament diameter can reduce that loss. However, as the filament diameter is reduced, other loss mechanisms increase in relative importance. The first estimate of coupling loss (at 50 percent of the correct value) was included in our modeling around 2010 and the corrected value was incorporated into our modeling in 2015. The transport current loss was not considered until 2016, but it is still thought to be small compared to the dominant hysteresis and coupling losses, unless there are magnetic components in the superconducting composite's matrix materials.

In summary, there are still considerable uncertainties and omissions in our AC loss treatment. As each of the increased loss estimates mentioned in the last paragraph came to our attention and were included in our analysis, it appeared that there were possible engineering solutions in wire configuration and constituent improvements (such as finer filaments, tighter twist, and higher matrix effective resistivity) in superconducting wire that could bring the losses down to a tolerable level. These engineering solutions to producing low-loss wire, as well as the heat transfer techniques for removing the losses from coils, still appear to be sufficient to cope with the losses. However, the near-term availability of these wire improvements was not a certainty and that meant that designing and testing a single 1-MW electric machine would not yet be a useful and cost-effective developmental path. A design was completed for a 1-MW machine, but current wire manufacturing constraints meant that this machine would not be prototypic of a high specific power design needed for future aircraft. Therefore, although it was still possible to design, build, and test a 1-MW machine, the research team recommended in 2016 that the better near-term research objective would be to build a test capability for superconducting coil test articles in an environment like that of a 1-MW superconducting electric machine. Subsequent sections examine the domestic MgB_2 wire manufacturing status and present the rationale for thinking that reasonably expected loss reductions and suitable heat transfer techniques can yield high-performance MW-class machines.

State of Development of MgB_2 Composite Wires

No existing application of superconducting wire has required that AC losses be as low as they will have to be in fully superconducting machines for the turboelectric aircraft application. It has therefore been necessary for NASA to support wire development starting from the state-of-the-art point where

losses were becoming low enough for ground applications at power line frequencies (60 Hz), but were not low enough for frequencies of several hundred Hz, which are expected in superconducting stators in airborne machines. As already noted, only MgB_2 is currently a viable candidate for the application of interest here.

Figure 6 shows a conductor typical of what was available commercially in 2006 from Hyper Tech, the only domestic manufacturer of MgB_2 wire. That wire contained 18 superconducting filaments of roughly 70 μm in diameter and was designed for use in magnetic resonance machines. The wire was essentially untwisted. Under Small Business Innovation Research (SBIR) grants, Hyper Tech developed MgB_2 wire with finer filaments and tighter twist pitch.

Filaments as small as 10 μm in diameter and twist pitch as small as 5 mm were produced. Compared to the original state of 70-μm filaments and essentially no twist, this was enormous progress. Figure 7 shows a cross section of a wire with 342 filaments produced by Hyper Tech (Tomsic et al., 2015). The pictured strand is of the so-called double-restack variety, made by first restacking 18 single strands together in an external tube, drawing that down and then restacking 19 of those together in another outer tube. The MgB_2 superconductor fraction in single-restack strands is about 12 percent and is reduced to about 7 percent in double-restack strands due to the extra tubes introduced. For the same size wire, the double restack can result in a wire with more and smaller filaments, but the current carrying capacity falls because of the smaller superconductor fraction.

Unfortunately, there were two problems with wires such as illustrated in Figure 1 and Figure 7 with respect to development of a fully superconducting, 1-MW electric machine. One problem was that this combination of matrix materials in the composite wire had a very low effective resistivity. This low electrical resistivity counteracted the coupling loss improvements made by producing a very tight twist. The second problem was that, in a single-restack configuration, the small filament size (10 μm) was achieved by drawing wires down to a total wire diameter of about 0.3 mm. The critical current of such a small wire (at 25 K and 0.5 T) is only about 20 A, and at a typical operating ratio of 50 percent, the useful operating current would be limited to only 10 A. That small current would require the motor to operate at a voltage too high to be practical.

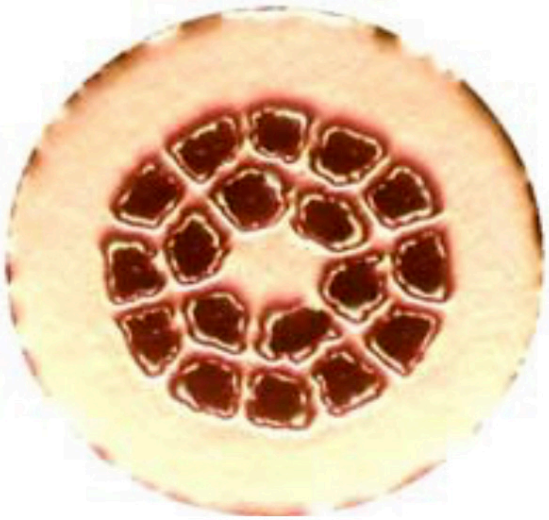

Figure 6.—Magnesium diboride commercial wire product before our Small Business Innovation Research (SBIR) grants. Sheaths around 18 MgB_2 filaments are Nb and remainder is copper.

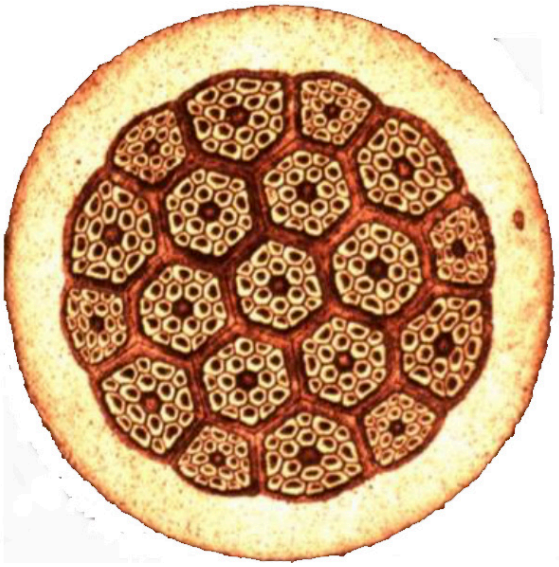

Figure 7.—Hyper Tech Research, Inc., produced MgB_2 strands like this one, which has 342 filaments. Wire diameter is 1 mm and filament diameter is ~13 μm.

Effective Transverse Resistivity of Composite Superconducting Wire

The problem of finding an effective transverse resistivity for the superconducting composite is difficult. The coupling loss is inversely proportional to the effective resistivity, as shown in Equation (4). Aside from this modeling issue, designing a wire to achieve a high transverse resistivity is complicated by the variety of materials required in the system and the fact that some of them have a very low resistivity. Each superconducting filament is surrounded by a pure Nb sheath that provides a barrier against diffusion of other elements into the superconductor during heat treatment. A tube of strong material that facilitates drawing the wire, typically an alloy of copper and nickel, surrounds the Nb in each single-filament strand, and a similar tube is added each time filaments are restacked to make a multifilament wire. As is illustrated in Figure 8(a), the superconducting filament together with its Nb sheath offer a very low resistance transverse path for eddy and coupling currents compared to the rest of the matrix material, and the currents deviate to flow through the filaments and Nb. The ratio of the effective resistivity to the matrix resistivity is given by Carr (2001) to be $(1 - \lambda)/(1 + \lambda)$ where λ is the volume fraction of low-resistivity material. For typical MgB_2 wire, λ is 0.45 resulting in the quoted ratio being 0.37. Thus, the effective resistivity is only 0.37 of the matrix resistivity, resulting in a coupling loss that is 2.6 times as much as it would be if the low-resistivity materials were not present.

If on the other hand, some way were developed to put an insulating barrier around the Nb, then the coupling currents would be forced to flow around the Nb, as illustrated in Figure 8(b). Carr quotes the ratio of effective resistivity to the matrix resistivity to be $(1 + \lambda)/(1 - \lambda)$ for this case. The effective resistivity would be 2.6 times the matrix resistivity and the coupling loss would be reduced to only 37 percent as much as it would be if the inclusions were not present. Unfortunately, no method is yet known for providing such a resistive barrier around the Nb sheaths.

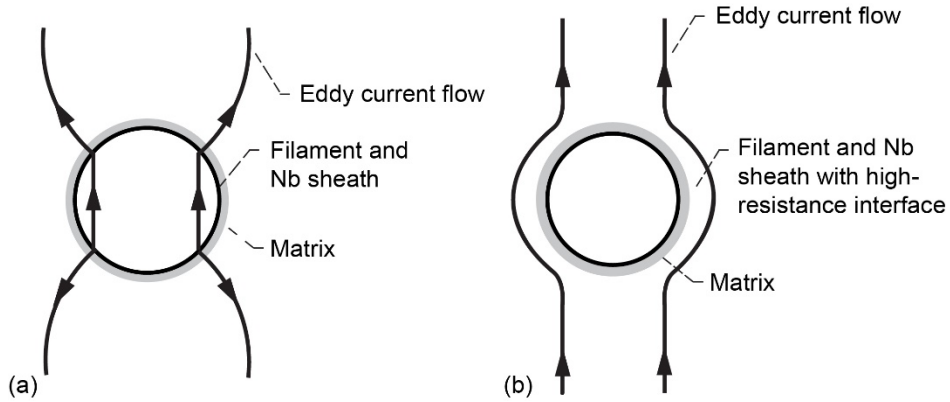

Figure 8.—Transverse currents in vicinity of high- and low-conductivity inclusions. (a) Inclusion has negligible resistivity compared to high-resistivity matrix and negligible interfacial resistance. Inclusion consists of superconducting filament plus surrounding pure Nb. (b) Very high interfacial resistance preventing current flow through Nb and superconductor. (Carr, 2001, p. 117).

Achieving Reasonably High Operating Current and Small Filaments in the Same Wire

The J_c in MgB_2 filaments can be very high. Based upon the authors' analytical fits to experimental data provided under the Hyper Tech SBIRs, and updated with more recent measurements at The Ohio State University, the dependence of J_c on T and applied B is given by

$$J_{c_{\text{filaments}}} = 8.49\left[\left(1.907T^2 - 121.5T + 2{,}027.9\right) - \left(1.0268T^2 - 64.14T + 1{,}116\right)\ln\left(B\right)\right] \tag{8}$$

for $0.2 < B < 2$ and $20 < T < 28$.

Figure 9 shows contours of this J_c in the filaments as functions of T and B. Considering a standard operating condition of 25 K and 0.5 T used previously, it can be seen from Figure 9 that at those conditions the filaments should have a J_c of about 2,400 A/mm^2. It may also be noted that, starting from 25 K and 0.5 T, a decrease of T by 5 K or a decrease of B to 0.1 T almost doubles the J_c of the filaments.

Of more practical interest is the J_c of an entire wire, which typically contains only 12 percent of superconductor by volume. In a steady-state situation, only the superconducting filaments carry current so the J_c of the wire is just that of the filaments multiplied by the volume fraction of superconductor. The wire J_c is shown in Figure 10 for a single-restack wire, such as the wire shown in Figure 1. At 25 K and 0.5 T, the figure indicates the wire J_c to be about 290 A/mm^2. This current density should be compared with what can be achieved in copper at room temperature: roughly 5 A/mm^2 in coils cooled by natural convection in air and perhaps 15 A/mm^2 with standard, noncryogenic, liquid cooling.

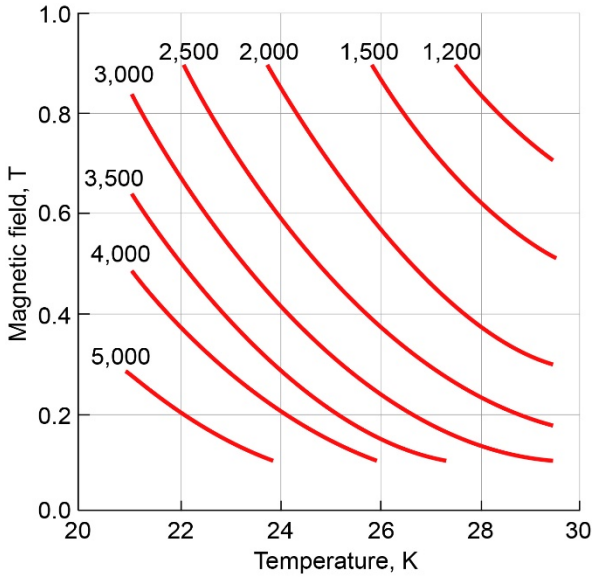

Figure 9.—Contours of critical current density in A/mm^2 of MgB_2 filaments as function of temperature and magnetic field.

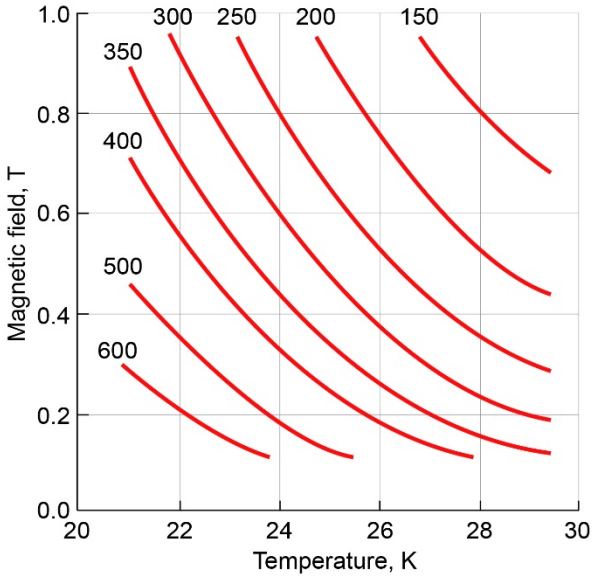

Figure 10.—Contours of critical current density in A/mm^2 in whole MgB_2 wire at 25 K and 0.5 T.

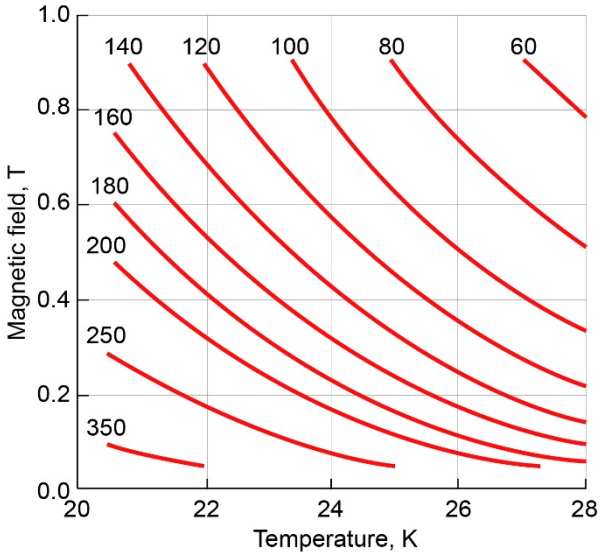

Figure 11.—Operating current in A of 1-mm-diameter MgB_2 superconducting wire of single-restack variety as function of temperature and magnetic field for operating ratio of 50 percent.

Consider now the total critical current that a wire can carry, as opposed to its current density. This is important because of how the current is related to the operating voltage of the electric machine and to the power converter connected to the machine. To allow a factor of safety, we typically choose an operating current that is only 50 percent of the critical current. A contour plot of the operating current for a wire of the single-restack variety is shown in Figure 11 for an operating ratio (ratio of current to critical current) of 0.5. From this figure, we see that at 25 K and 0.5 T a MgB_2 wire that is 1 mm in diameter can carry about 115 A, operating at 50 percent of its critical current. Unfortunately, at this wire size the superconducting filaments may not be small enough for tolerable hysteresis loss based on demonstrated manufacturing processes.

To consider both wire and filament constraints, we need a relation between filament size, wire size, superconducting packing fraction, and the number of filaments. This can be obtained by noting that the product of wire cross-sectional area and the volume fraction of superconductor must be equal to the number of superconducting filaments times the cross-sectional area of one filament. That leads to the following relation:

$$\frac{d_f}{d_{\text{wire}}} = \left(\frac{\lambda}{N_{\text{filaments}}} \right)^{1/2} \tag{9}$$

where d_f is the filament diameter, d_{wire} is the wire diameter, and $N_{\text{filaments}}$ is the number of filaments in the wire. By using that relation and Equation (8), we can plot a combined graph of operating current and filament diameter as functions of wire diameter. Figure 12 shows these quantities for single-restack wires (such as pictured in Figure 1) and for double-restack wires (such as pictured in Figure 7). To relate filament size to wire size, we have to pick the number of filaments in the wire, which can vary widely, and we have to choose between single restack and double restack. For definiteness in Figure 12, we have used one single-restack wire with 114 filaments, another single-restack wire with 180 filaments and a double-restack wire with 342 filaments. It can be seen from the two dashed red lines (114 and 180 filaments and right scale) that, for a fixed wire diameter, increasing the number of filaments can keep the

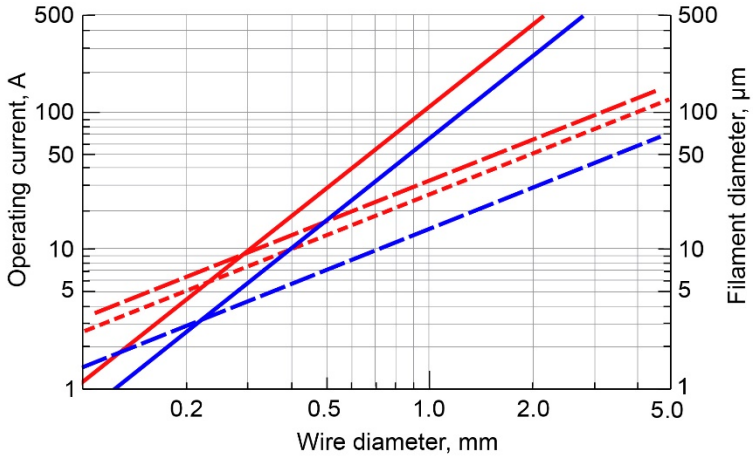

Figure 12.—Operating current (left scale, solid lines) and filament diameter (right scale, dashed lines) as functions of wire diameter at 25 K and 0.5 T for operating ratio of 50 percent. Red lines are for single-restack wire and blue lines are for double-restack wire. Long-dashed red is for 114 filaments and short-dashed is for 180 filaments, both with superconductor volume fraction of 12 percent. Blue dashed line is for 342 filaments and superconductor volume fraction of 7 percent.

operating current (solid red line and left scale) the same while reducing the filament size. Each of these filament counts has been successfully manufactured by Hyper Tech Research, Inc.

For a given wire diameter and current manufacturing process, a double restack has less current capacity than a single restack (independent of filament number), but if the double restack has more total filaments, the filaments will be smaller and yield less hysteresis loss.

It may be feasible to safely operate AC stator coils with a current amplitude that is greater than 50 percent of the critical current. See the relevant discussion of appropriate definition of critical current in an AC situation in Lee and Ko (2014). In a DC condition, when the current exceeds the local critical current I_c by a given amount (say 10 percent), there is a local heat production related to that steady excess of current. However, in an AC situation, when the current amplitude exceeds I_c by the same given amount (10 percent), the dissipation occurs only for the portion of the cycle when the current is above I_c, so the produced heat may be removable by available heat transfer and prevent a runaway warmup.

Heat Removal Capability

No means of power conversion can be accomplished without some losses and, therefore, heat generation. Thermal management of AC losses in a superconducting electric machine system by a flowing coolant will now be considered briefly. To begin, the losses presented in Figure 5 on a volumetric basis are here recast into loss per unit surface area of a 0.96-mm-diameter wire in Figure 13. The surface heat flux is then 0.04 W/cm^2 for the standard temperature field condition (25 K and 0.5 T) and wire with 31-µm filaments and a twist pitch of 5 mm. This surface heat flux is the heat that must be removed, either directly to a coolant or through some intervening medium and eventually to a coolant fluid. Optimization of the cooling method is beyond the scope of this report, but two example illustrative cases will be considered: (1) wires in direct contact with fluid (Figure 14) and (2) wires potted in epoxy (Figure 15 and Figure 16). At first, we consider the fluid to be nonboiling liquid hydrogen. Such a cooling scheme would be appropriate in a liquid-hydrogen-fueled aircraft or on a jet-fueled aircraft that carries enough liquid hydrogen inventory for cooling superconducting machines and other cryogenic electric components such

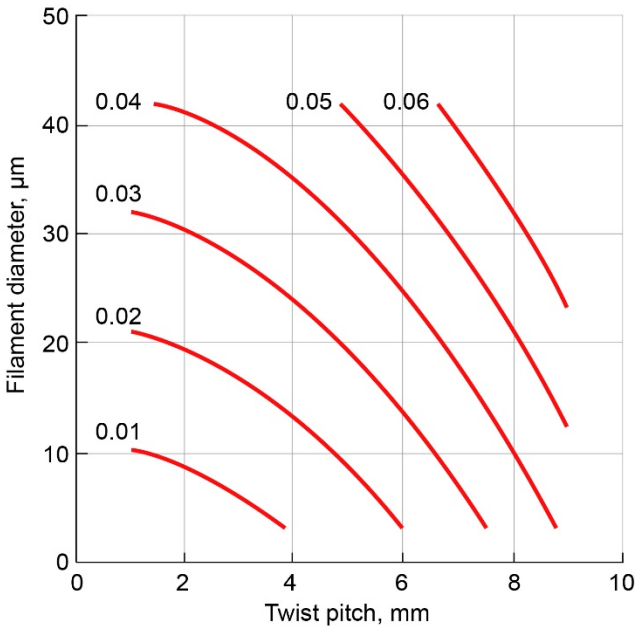

Figure 13.—Wire surface heat flux in W/cm^2 as function of twist pitch and filament diameter.

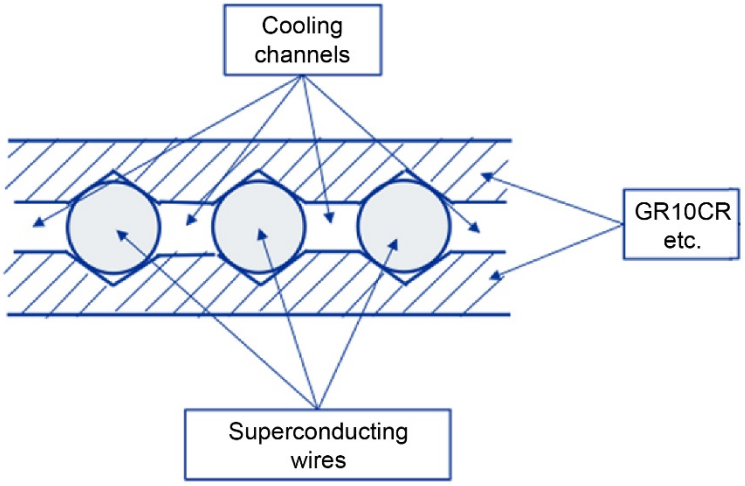

Figure 14.—Portion of stator coil straight section, seen in cross section. Individual wires are separated by insulating former pieces above and below wires. Coolant channels between wires are shown as roughly square. We chose side of square to be 0.7 mm for of 0.96-mm-diameter wires. Wire must run only 0.15 K hotter than fluid to reject heat from AC losses for our standard operating case.

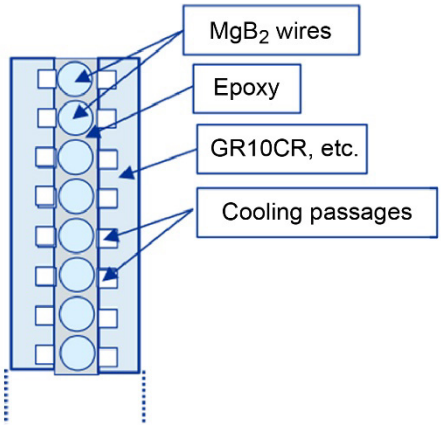

Figure 15.—Single layer of MgB_2 wire embedded in epoxy. Wire spacing is very small in comparison to wire diameter. Minimum distance from wire surface to epoxy surface is assumed to be 0.1 mm. Effective average heat transfer distance from wire to epoxy surface is taken as 0.3 mm. Wire must run 1.46 K hotter than bulk coolant temperature for our standard operating case.

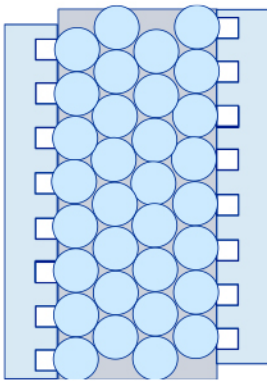

Figure 16.—Four-layer coil with hexagonal close packing in limit of zero spacing between wires. Wire must run only 1.88 K hotter than fluid, an acceptable value if zero spacing were physically achievable.

as cryogenic power converters (Felder, Kim, and Brown, 2009). For these cooling calculations, we do not consider transient effects, and it is always assumed that the hydrogen is under sufficient pressure to prevent boiling in the cooling channels. Superconducting machines cooled by cryocoolers were also studied in Felder, Kim, and Brown (2009) and Brown (2011). Pressurized helium gas would be the coolant medium for superconducting machines in that situation. We use the equations shown in Appendix C for heat transfer.

The goal of the heat transfer analysis is to be sure that the temperature differences necessary to transfer the heat are not large enough to impair the current carrying capacity of the superconductor.

The estimates of the required temperature rise of the wire above the temperature of the flowing coolant and of the required pumping power to circulate the fluid suggest that it is feasible to cool bare superconductor and epoxy-encapsulated coils up to a few layers thick. In the direct cooling case of Figure 14, the wires operate at a temperature only 0.15 K hotter than the flowing liquid hydrogen. In the single-layer coil of Figure 15, the wires run 1.5 K hotter than the hydrogen, and in the four-layer limiting case in Figure 16, which is physically unrealizable as the wires are in direct contact with each other, the wires run 1.9 K hotter than the fluid. In all cases, the fluid in a cooling channel heats up by a manageable amount and the pumping power to force the fluid through the submillimeter-sized cooling channels is also acceptable. See Appendix D for more discussion, including two- and four-layer epoxied coils with realistic spacing.

In summary, up to four-layer epoxied coils may be feasible with liquid hydrogen as a coolant, especially if the thermal conductivity of the epoxy can be improved with fillers.

Comparison of MgB_2 Losses With Copper Wire Losses

The various superconductor AC losses add up to a total today that is considerably larger than previously expected. It is fair to ask if the superconductor actually has a significant advantage over a simple copper wire winding at room temperature or one that is cryogenically cooled. To answer that question, wire loss comparisons were made using fixed analysis values of 0.96 mm wire diameter, 100 A

operating current, 0.5 T externally applied AC field strength, and 200 Hz AC frequency. The losses were compared for single-strand copper wire operating at room temperature, single-strand copper wire operating at 20 K, copper Litz (commercially available multistrand and twisted) wire operating at 20 K, MgB_2 wire that is available today, and MgB_2 with a higher resistivity matrix. The results are shown in Figure 17 and Figure 18. Figure 17 shows that the loss in room temperature copper at this AC density (138 A/mm^2 amplitude) would be extremely high at 163 W/cm^3, 162 of which is Joule (I^2R) heating and 0.67 W/cm^3 is eddy current heating due to the AC applied field. (See Appendix E for the general equation for eddy current loss of a conductor in a perpendicular AC field.) If the same copper wire (with an assumed residual resistivity ratio of 100) were operated at 20 K, the Joule heating would drop to only 1.63 W/cm^3. However, magnetoresistance comes into play slightly for high-conductivity copper at 20 K (see Appendix F), adding about 12 percent to the resistance, and raising the Joule heating to 1.82 W/cm^3. The solid wire is subject to an even larger penalty from eddy current heating, which would add 53 W/cm^3 for a total of 55 W/cm^3 (see Appendix E.) The common method of reducing eddy current loss is to use Litz wire, so a Litz wire bundle with 70 percent copper packing fraction that is 0.96 mm in overall diameter and composed of filaments that are 0.1 mm in diameter (#38 wire) is the next case. The AC current must still have 100 A amplitude, so the current density goes up, increasing the Joule loss to 2.61 W/cm^3. The eddy current loss is reduced to 0.65 W/cm^3 for a total of 3.26 W/cm^3. Figure 18 expands the last three bars of Figure 17 for better comparison.

Next consider the MgB_2 wire that is available today at a diameter of 0.96 mm, which has filaments of 31 μm diameter, twisted with a pitch (360°) of 5 mm. That wire has a predicted loss of 1.7 W/cm^3, as could be seen from Figure 5, which is reproduced as Figure 19 with the wire under discussion shown in the figure by the open-circle data point. The loss is shown in Figure 18 as well.

Such a wire could be drawn to a smaller diameter (~0.33 mm) to yield filaments as small as 10 μm diameter, but then the wire operating current would be only about 10 A. The losses per unit volume for such a wire are predicted in Figure 19 by the filled-circle data point to be about 0.9 W/cm^3. Cabling 7 of those wires together would yield a cable of approximately 0.96 mm in diameter, but would not quite recover the desired 100 A operating current. Increasing the operating fraction (fraction of critical current) to 70 percent from 50 percent, would give 100 A.

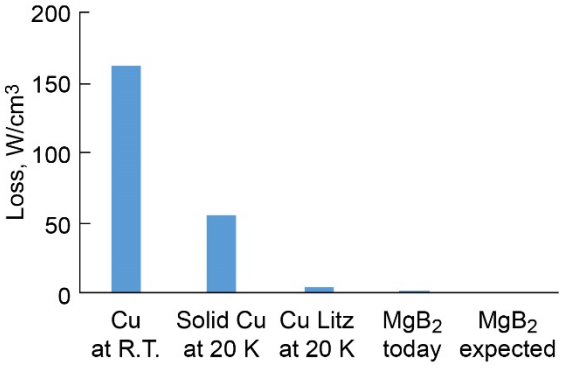

Figure 17.—Losses in various copper and MgB_2 wires. All wires are 0.96 mm in diameter and carry 100 A operating current in an AC magnetic field of 0.5 T at 200 Hz. Solid copper case at 20 K includes 12 percent magnetoresistance plus large eddy current loss. Copper Litz wire has 100-μm filaments. Room temperature (R.T.).

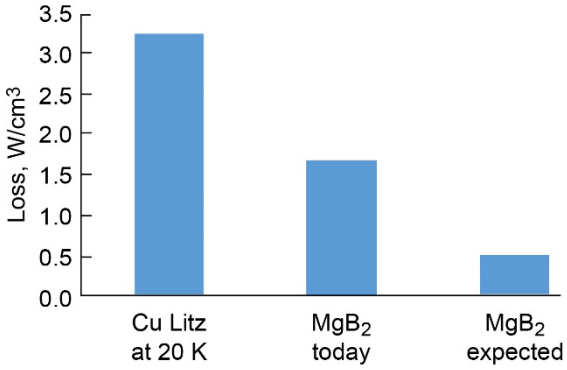

Figure 18.—Losses of cryogenic copper Litz wire and MgB_2 wires.

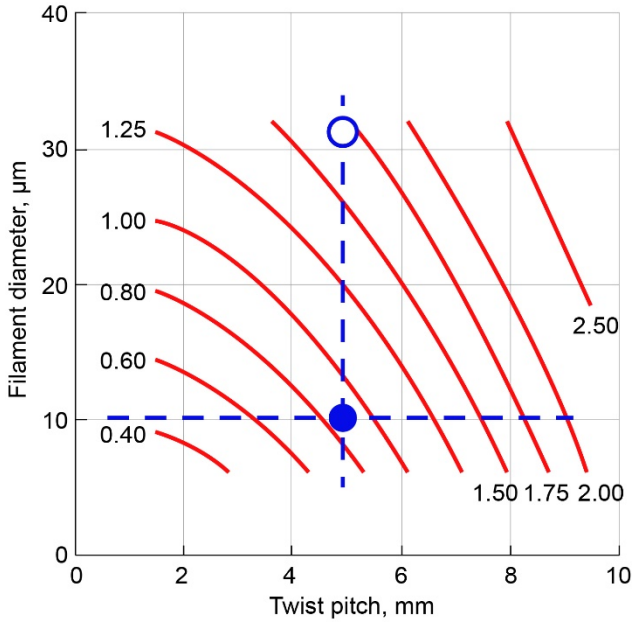

Figure 19.—Volumetric losses for strands of MgB_2 highlighting two examples of wire with 5-mm twist. Open circle represents our current "standard" wire. Filled circle represents same wire at smaller diameter, but with same twist. T = 25 K. B = 0.5 T. Superconducting fraction = 0.12.

Next consider that cabled wire further, but suppose that it becomes possible in the future to increase the effective matrix resistivity to 50 μΩ·cm. That would drop the total AC loss to 0.5 W/cm^3.

In the cabled cases, we ignore the cabling AC loss, which is considered to be easily controlled to a low level by the MgB_2 specialist Michael Sumption of The Ohio State University who measures the Hyper Tech wire properties. Cabling is being explored in a Phase II SBIR as of April 2019.

In summary, it is clear that MgB_2 wire is far superior to copper with respect to low losses in a machine stator, whether the copper is at room temperature or cryogenically cooled. What we have not shown in this report is the feasible packing fraction of the various conductors in a winding. In the case of the superconductor winding, the coil formers, which provide conductor support and configure the cooling channels, may take up a large fraction of the winding space. For copper windings, the coil formers might be comparatively minimal, but the large amount of heat to be removed may require considerable space for cooling channels. All of these tradeoffs need further refinement, but the fundamental driver of superconducting machines is the potential for achieving the loss reductions represented in Figure 18.

Possibility of Round-Wire High-Temperature Superconductors

At present, the only multifilament superconductor that can be practically manufactured in round wire form with fine filaments is MgB_2, which has a critical temperature of 39 K and must be operated below 30 K to have reasonably high current carrying capacity. It has been speculated since the outset of this project that another of the HTS materials, for example, bismuth strontium calcium copper oxide 2212 (BSCCO 2212) with a critical temperature 95 K, could be developed in round-wire form, and sizing model calculations have been carried along for such a hypothetical future material as well (Felder, Kim, and Brown, 2009, and Brown, 2011). There have been developments in the last 2 or 3 years that revive this hope. BSCCO 2212 processing at moderately high pressure has yielded wire that has six times the critical current density (at 4.4 K and high magnetic fields on the order of 10 T) of previously produced

material, (Larbalestier, 2016). See Figure 1 of Chen et al. (2016) for a micrograph of the cross section (prior to heat treatment) of a 1.3-mm-diameter wire that has been produced with 2,178 filaments of BSCCO 2212. Note that this wire has finer filaments and hence many more filaments for roughly the same wire diameter than have been produced in MgB_2 to date. If similar improvement factors in critical current hold for temperatures in the range of 20 to 50 or 60 K and at low fields (~1 T or less), then the outlook for a low loss AC superconductor may have been greatly improved. Three possible problems to be noted for BSCCO 2212, however, are (1) the amount of silver required to surround the superconducting filaments, (2) the low resistivity of that material, and (3) the tendency of the BSCCO 2212 to form whiskers during heat treatment that provide current paths between filaments and hence high coupling losses. A NASA Phase I SBIR "Bi2212 superconductors for high-power density motors for aero propulsion" was awarded to Solid Material Solutions, LLC, in 2018 to study this material. Results are described in the Phase I Final Report (Solid Material Solutions LLC, 2019), which is not yet publicly available under SBIR rules.

Concluding Remarks

Over several years, our predicted superconductor alternating current (AC) losses grew from a very tolerable level to a level that presented concerns with respect to thermal management of the losses. The reasons for the worsening outlook varied from an initial lack of appreciation for the higher frequencies required in the aircraft to errors in the coupling loss formula. In any case, there was a progression in the analytical expressions we used to estimate AC losses, and every change resulted in higher predicted loss.

On the wire fabrication side, some of the difficulties in manufacturing MgB_2 wire were not apparent to Glenn Research Center until recently, and the issues with forming the wire into usable machine coils were not appreciated. Hyper Tech Research, Inc., did not make fine-filament, tightly twisted wire before our Small Business Innovation Research (SBIR) grants, which began in 2009 and 2012. During those SBIR grants, the firm reduced superconducting filament diameter from 70 μm or more to as small as 10 μm and reduced the twist pitch from about 200 to 5 mm. These improvements far exceeded our expectations for the timeframe. However, being able to draw wire with such fine filaments and tight twist depended upon having a metallic matrix that was reasonably ductile. Unfortunately, good ductility does not correspond to high electrical resistivity, which is needed for low coupling loss. The present effective matrix resistivity is about 1/8 of our original assumption, leading to an expected coupling loss nearly an order of magnitude higher than initially expected.

On the brighter side, there are some developments that may lead to lower AC losses and to higher critical currents. A second-generation synthesis process for MgB_2 gives three or more times as much critical current density as the first-generation process. Higher critical current density cannot reduce the hysteresis loss as a fraction of the machine output power, but it would reduce the coupling loss relative to hysteresis loss because the amount of normal matrix in the superconductor is reduced in proportion to the total amount of superconductor, which goes down inversely with critical current. The specific power would thereby increase as well as the efficiency.

Our view of the possibility of achieving adequate cooling without spoiling the engineering current density, and hence the specific power, went from being very optimistic several years ago to rather pessimistic as the AC loss estimates rose. However, the specific examples considered herein suggest that, even with the MgB_2 wire that can be made today, adequate cooling should be possible in epoxy-potted coils. Some approach may become feasible for potting the superconducting wire in an epoxy that is filled with a higher thermal conductivity material. The use of other high-thermal-conductivity materials may be possible, such as grown sapphire, perhaps in fiber or woven-tape form. In all the approaches to improve

heat removal, the specific power (which this report did not attempt to evaluate) may suffer to some degree, but it has been pointed out (Jansen, 2015) that high powertrain efficiency has a greater benefit than very high specific power when the overall aircraft is considered. This report showed that the efficiency achievable by the superconducting approach cannot likely be matched with room temperature electric machines wound with copper conductor.

So in spite of the increases in predicted AC losses that we have discussed, it appears that superconducting AC windings can still be cooled adequately. Thus, very high efficiency fully superconducting machines still appear to be obtainable. The very favorable comparison that was presented between AC losses in currently available MgB_2 wire (1.7 W/cm^3) and copper at room temperature (163 W/cm^3), solid copper at 20 K (54 W/cm^3), copper Litz wire at 20 K (3.26 W/cm^3), and expected future MgB_2 wire (0.5 W/cm^3) provides the motivation for this superconductor work and is the justification to continue it.

Appendix A.—Proportionality of Hysteresis AC Loss and Produced Power

Let the machine with active length L have p pole pairs. We neglect both the torque and the losses in the end turns of the machine. We also neglect the magnetic field B contributed by the stator itself. Let the three-phase armature be thin compared to its average radius r. Assume that the field B from the rotor is sinusoidal with amplitude B_0 around the circumference measured by the physical angle θ, and let the current density per unit width λ(θ) in each phase be sinusoidal in θ with amplitude λ_0:

$$B(\theta) = B_0 \sin(p\theta)$$
$$\lambda_n(\theta) = \lambda_0 \sin\left(p\theta + \frac{2n\pi}{3} + \varphi\right) \tag{A1}$$

$$\lambda(\theta) = \left(\frac{3\lambda_0}{2}\right)\sin(p\theta) \tag{A2}$$

where p is the number of pole pairs, n enumerates the phases, and φ is the appropriate phase angle to make the three-phase total current in phase with the rotor magnetic field. Equation (A2) will be different for typical real windings with winding distributions that are constant over various intervals rather than sinusoidal. For distributed current, the incremental circumferential force dF due to an increment of current dI, considering all three phases working together, will be

$$\begin{aligned} dF &= LB(\theta)\,dI \\ &= LB(\theta)\lambda(\theta)\,r\,d\theta \\ &= \left(\frac{3\lambda_0}{2}\right)LB_0 r \sin^2(p\theta)\,d\theta \end{aligned}$$

where the factor of 3/2 comes from the fact that the amplitude of the traveling wave that is the sum of three standing sine waves that are 120° out of phase is 3/2 of the amplitude of the constituent sine waves. Integrating with respect to θ gives the total circumferential force and noting that the integral of $\sin^2(p\theta)$ from 0 to 2π is π, the circumferential force is obtained:

$$F = \frac{3\pi}{2} B_0 \lambda_0 L r$$

Then the torque $T = rF$ will be

$$T = \frac{3\pi}{2} B_0 \lambda_0 L r^2$$

and the shaft power $P_s = f_s T$, where f_s is the rotational frequency of the shaft, will be

$$P_s = \frac{3\pi}{2} B_0 \lambda_0 L r^2 f_s \tag{A3}$$

Now consider the hysteresis loss in the entire armature. We have an expression for the hysteresis loss P_h from Equation (4):

$$P_h = \frac{4}{3} J_c B_0 d_s f_e V_{\text{filaments}} \tag{A4}$$

where J_c is the critical current density in a filament, d_s is the superconducting filament diameter, f_e is the electrical frequency, and $V_{\text{filaments}}$ is the total volume of all the filaments in the active length of the machine. We need to find the total filament volume in the active length of the machine.

Note that we have been using the current per unit width in one phase previously. That quantity divided by the filament current density J_{fil} would give the filament cross-sectional area A_{fil} in one phase per unit width (at the armature radius r and as a function of θ):

$$A_{fil}(\theta) = \frac{\lambda_0}{J_{fil}} \left| \sin(p\theta) \right|$$

where the absolute value is required because the same amount of superconductor is required regardless of the sign of the current. Now reintroducing the operating ratio $\gamma = J_{fil}/J_c$, we can write the current per unit width in one phase at r as

$$A_{fil}(\theta) = \frac{\lambda_0}{\gamma J_c} \left| \sin(p\theta) \right|$$

The total filament volume in three phases is then $3L\int A_{fil}(\theta) r d\theta$, and noting that $\int \left| \sin(p\theta) \right| d\theta$ from 0 to 2π is 4,

$$V_{\text{filaments}} = 3rL\left(\frac{\lambda_0}{\gamma J_c} \right) 4 = \frac{12\lambda_0 rL}{\gamma J_c}$$

and substituting that result into Equation (A4) gives

$$P_h = \frac{16 B_0 d_s f_e \lambda_0 rL}{\gamma}$$

Noting now that $f_e/f_s = p$, we can write the quotient of P_h/P_s as

$$\frac{P_h}{P_s} = \frac{32}{3\pi} \frac{p}{\gamma} \frac{d_s}{r}$$

It is interesting to note that neither the field strength nor the superconductor J_c has any effect on this quotient. Once the number of pole pairs p and the operating ratio γ are chosen, the fractional hysteresis loss depends only on the ratio of the superconducting filament size to the radius of the armature.

Current distributions other than sinusoidal will change the numerical prefactor, but not the functional dependence on the parameters.

Appendix B.—Ratio of Coupling Loss to Hysteresis Loss

From Equations (3) and (4) we have the following for the time-averaged coupling loss power P_c and the time-averaged hysteresis loss power P_h in an AC situation P_h:

$$P_c = \frac{1}{2\rho_{eff}}\left(B_0 L_t f_e\right)^2 V_{\text{matrix}}$$

$$P_h = \frac{4}{3} J_c B_0 d_s f_e V_{\text{filaments}}$$

where B_0 is the magnetic field, L_t is the twist pitch of the filaments, f_e *is* the electrical frequency, ρ_{eff} is an effective transverse resistivity of the metals in the crossover regions, V_{matrix} is the volume of the nonsuperconducting part of the composite, d_s is the superconducting filament diameter, J_c is the critical current density in the superconducting filaments, and $V_{\text{filaments}}$ is the volume of the superconducting filaments only.

The two equations can be put on the same volumetric basis by assuming that the volume fraction of superconductor is α. Then $V_{\text{filaments}} = \alpha V_{\text{wire}}$ and $V_{\text{matrix}} = (1 - \alpha)V_{\text{wire}}$. Then the ratio of coupling loss to hysteresis loss is

$$\frac{P_c}{P_h} = \frac{\left(\frac{1}{2\rho_{eff}}\right)\left(B_0 L_t f_e\right)^2 (1-\alpha)}{\left(\frac{4}{3}\right) J_c B_0 d_s f_e \alpha}$$

$$= \frac{\left(\frac{3}{8}\right)\left[\frac{(1-\alpha)}{\alpha}\right] B_0 f_e L_t^2}{J_c d_s \rho_{eff}}$$

Appendix C.—Heat Transfer and Fluid Flow Equations

To estimate the superheat of the solid surfaces above the temperature of the bulk flowing fluids (liquid hydrogen or gaseous helium), we use the following relations.

Prandtl Number Pr is

$$\mathrm{Pr} = C_p \, \mu / k$$

where C_p is the fluid's heat capacity at constant pressure, μ is the fluid's dynamic viscosity, and k is the fluid's thermal conductivity.

Reynolds number Re is

$$\mathrm{Re} = \rho v D / \mu$$

where ρ is the fluid density, v is the fluid bulk velocity, and D is the hydraulic diameter of the flow passage.

The Nusselt number Nu, to be found using a correlation given below, is defined as

$$\mathrm{Nu} = hD/k$$

where h is the convective heat transfer coefficient.

To find the Nu for turbulent flow, we use the Dittus-Boelter correlation (Incropera, 2007) for smooth round tubes for heating of the fluid:

$$\mathrm{Nu} = 0.023 \mathrm{Re}^{0.8} \, \mathrm{Pr}^{0.4}$$

which is applicable in the range $0.6 < \mathrm{Pr} < 160$ and $\mathrm{Re} > 10{,}000$. Our conditions for both liquid hydrogen and gaseous helium satisfy those conditions.

To calculate pressure drop and pumping power we use the following equations.

Pressure drop ΔP in a channel of length L and hydraulic diameter D and Darcy friction factor f for the fluid of density ρ flowing with velocity v is calculated from

$$\Delta P = \frac{f L \rho v^2}{D}$$

The Darcy friction factor is given by

$$f = 0.316 / Re^{0.25}$$

valid for $\mathrm{Re} > 3{,}000$.

Pumping power P_{pumping} is then $P_{\mathrm{pumping}} = v \Delta P$.

Appendix D.—Heat Removal

First, we consider a case where the fluid flows parallel to the wires and between them with the wire separation determined by spaced grooves in two solid insulating formers on either side of the winding layer, as shown in Figure 14. We consider only the long straight sections of a stator racetrack coil or a saddle coil, which are presumed to be long enough that the end turns are in a weak enough field that the heat transfer is significantly less problematic. For the standard wire and conditions that we have used as an example in this report, the volumetric AC loss is 1.7 W/cm^3 of wire. For the 0.96-mm-diameter wire, this amounts to 0.0123 W/cm of wire length and 0.0408 W/cm^2 of wire surface. If 40 percent of the surface of each wire is exposed to the flowing coolant, the heat flux required from the cooled surface is 0.102 W/cm^2. We assume each metallic wire is isothermal. We assume the hydraulic diameter d_h of the roughly square cooling channel is 0.7 mm and note that the Prandtl number for liquid hydrogen at our conditions is 1.125. Then for an example mass flow rate of 0.08 g/s, which results in a flow velocity of 2.94 m/s and a Reynolds number of 10,800, the turbulent flow Nusselt number Nu predicted by the Dittus-Boelter correlation (Incropera et al., 2007) is 40.6. Then the heat transfer coefficient is $k\mathrm{Nu}/d_h$ = 6,955 W/(K·m^2) (where k is thermal conductivity of liquid hydrogen) and the surface superheat above the bulk liquid hydrogen temperature is only 0.15 K, a very modest number. The superconducting wire runs only 0.15 K hotter than the fluid. For the relevant friction factor of 0.031, the pressure drop along a channel of 0.2-m length is 2,700 N/m^2 (0.39 psi), a moderate pressure drop, requiring 0.00306 W of pumping power per channel, which is only 1.24 percent of the 0.246 W of heat absorbed in the channel, an almost negligible efficiency impact to affect the removal of the AC loss. From inlet to outlet of the channel, the liquid hydrogen warms at most by 0.308 K (if we assume the same superconductor loss rate at all points along the channel), requiring only 20 psi of pressure to prevent boiling and avoid two-phase flow.

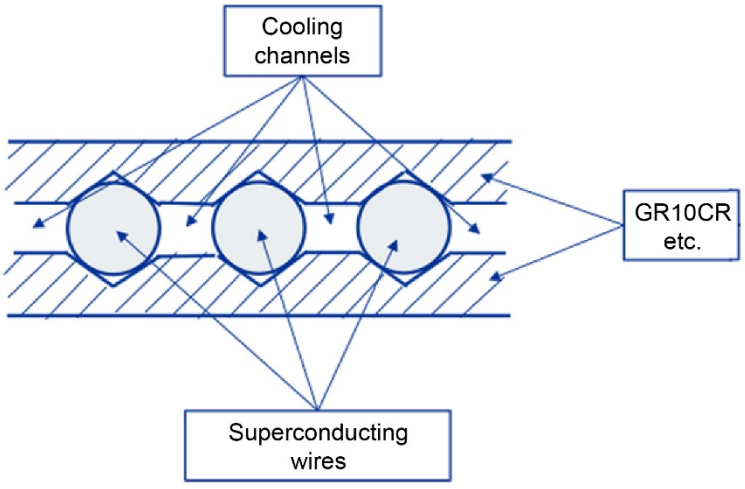

Figure 14.—Portion of stator coil straight section, seen in cross section. Individual wires are separated by insulating former pieces above and below wires. Coolant channels between wires are shown as roughly square. We chose side of square to be 0.7 mm for wires of 0.96-mm diameter. Wire must run only 0.15 K hotter than fluid to reject heat from AC losses for our standard operating case.

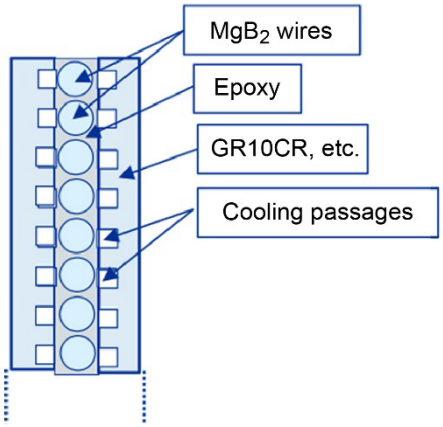

Figure 15.—Single layer of MgB_2 wire embedded in epoxy. Wire spacing is very small in comparison to wire diameter. Minimum distance from wire surface to epoxy surface is assumed to be 0.1 mm. Effective average heat transfer distance from wire to epoxy surface is taken as 0.3 mm. Wire must run 1.46 K hotter than bulk coolant temperature for our standard operating case.

Next, we consider whether epoxy-potted coils can be adequately cooled. Consider a single layer of MgB_2 wire embedded in epoxy and cooled on both sides as illustrated in Figure 15. This configuration has two cooling channels per wire as opposed to only one in the previous case. We assume in all the epoxied coil cases that there are no cracks between the wires and the epoxy and no surface thermal resistance between wire and epoxy. The wire spacing is taken as very small in comparison to the 0.96-mm wire diameter. The minimum distance from wire surface to epoxy surface is assumed to be 0.1 mm. The effective average heat-transfer distance from the wire to the epoxy surface is taken as 0.3 mm. We suppose the wire surface heat flux is the same as considered above, that is 0.0408 W/cm^2. The ratio of wire surface area to the epoxy's cooled-surface area is $\pi/2$ for negligible wire spacing. Then for an assumed epoxy thermal conductivity at 20 K of 0.15 W/(m·K), the wire temperature must be 1.28 K hotter than the epoxy surface to transfer the heat. Supposing that 50 percent of the epoxy surface is exposed to the liquid hydrogen flow in the multiple cooling channels and that the mass flow rate per channel is maintained at 0.08 g/s, we follow the same process as above to find that the epoxy surface will be 0.18 K warmer than the bulk liquid hydrogen temperature, a slightly higher surface-to-fluid value than in the previous case. The superconducting wire is 1.47 K hotter than the fluid, most of that value stemming from heat transfer through the epoxy. This is still a reasonable value. The liquid hydrogen warms by only 0.154 K from inlet to outlet as it absorbs the losses without boiling. This is half the warmup of the previous case because there are two cooling channels per wire instead of one.

Consider next, two layers of MgB_2 wire embedded in epoxy and cooled on both sides as illustrated in Figure D1. The wire spacing is again taken as very small in comparison to the wire diameter. The minimum distance from wire surface to epoxy surface is assumed to be 0.1 mm. The effective average heat transfer distance from the wire to the epoxy surface is still 0.3 mm because the heat can travel inside each wire to the side of the wire nearest to an epoxy surface with little temperature change. For two layers, the ratio of wire surface area to the epoxy surface area is π for negligible wire spacing. All the heat from a layer must travel in the same direction to reach a cooled surface, so the wire temperature must

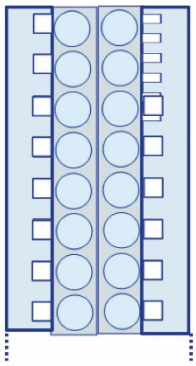

Figure D1.—Two layers of MgB_2 wire embedded in epoxy. Wire spacing is very small in comparison to wire diameter. Minimum distance from wire surface to epoxy surface is assumed to be 0.1 mm. Effective average heat transfer distance from wire to epoxy surface is taken as 0.3 mm. Wire must run 2.74 K hotter than fluid.

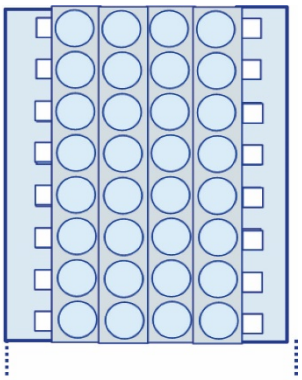

Figure D2.—Four layers of MgB_2 wire embedded in epoxy. Wire spacing is very small in comparison to wire diameter. Minimum distance from wire surface to epoxy surface is assumed to be 0.1 mm. Inner layers will run hotter than outer layers because of larger effective average heat transfer distance from wires to epoxy surface. Wire must run more than 15 K hotter than fluid, an unacceptable value.

be 2.56 K hotter than the epoxy surface to transfer the heat. Twice as much heat to reject as the previous case results in twice the surface superheat or 0.37 K. The superconducting wire must be 2.93 K hotter than the fluid. This is still a fairly reasonable value. The liquid hydrogen warms by 0.308 K from inlet to outlet, a moderate value.

Consider next, four layers of MgB_2 wire embedded in a square-packed array in epoxy and cooled on both sides as illustrated in Figure D2. The effective average heat transfer distance from the outer wires to the epoxy surface is still 0.3 mm but the heat from the inner layers has to travel through a greater distance in the epoxy, which we estimate (without analysis) to be 0.9 mm because the heat from the inner layer will travel as much as possible through the metallic wire of the outer layer in preference to the epoxy because of the higher thermal conductivity. Nevertheless, this larger effective distance through the epoxy has a devastating effect. For four layers, the ratio of wire surface area to the epoxy surface area is 2π. Now the wire temperature must be 15 K hotter than the epoxy surface to transfer the heat. This is an absolutely prohibitive value, since liquid hydrogen boils at 20.4 K and the critical temperature of MgB_2 in zero field is only 39 K. So four-layer coils are not possible in this configuration unless the thermal conductivity of the epoxy is improved nearly an order of magnitude by filling with high thermal conductivity particles such as sapphire or possibly with metallic particles that are so fine that their eddy current losses are not an issue.

The four layer case is somewhat improved if the wires could be packed in a close-packed arrangement as shown in Figure D3. The effective average heat transfer distance through the epoxy from the inner wires to the cooled surface is estimated to be about 0.6 mm, or about 2/3 that of the previous case. This reduces the inner wire temperature to only about 10 K hotter than the epoxy surface. This is still a prohibitive value unless improved thermal conductivity can be achieved by using higher conductivity fillers.

In Figure 16 is shown a limiting case with the best possible cooling for the inner layers of a four-layer coil potted in epoxy. The outer layer of wires is presumed to have 20 percent of its surface directly exposed to the coolant in the channels,which is similar to Figure 15, except that cooling is on one side only. There are assumed to be no gaps between the close-packed wires, so this case presents the minimum possible difference of temperature between the wires in the two layers. Since the wires must be

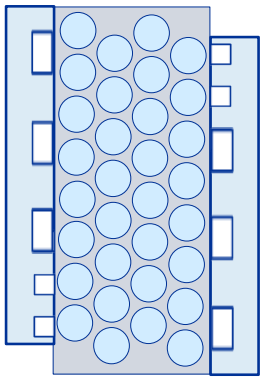

Figure D3.—Four-layer coil with hexagonal close packing, but nonzero spacing between coils. Wire must run about 10 K hotter than fluid.

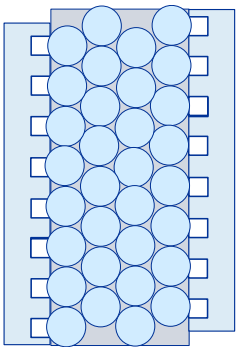

Figure 16.—Four-layer coil with hexagonal close packing in limit of zero spacing between wires. Wire must run 1.88 K hotter than fluid, an acceptable value if zero spacing were physically achievable.

electrically insulated from each other, this case is a non-achievable, ideal limit. We suppose that the effective average distance that heat must travel through epoxy between inner-layer and outer-layer wires is 1 mm, which is the same as the effective distance assumed in the geometry pictured in Figure 16. (An actual two-dimensional heat transfer calculation should be done to check the accuracy of this estimate.) Then the inner layer of wires will run only 1.28 K hotter than the outer layer of wires. The heat transfer from the outer wires to the coolant will require a higher superheat than for the Figure 15 case for two reasons. The wire exposure to coolant is only half as much and the heat to be transferred is twice as much. Hence the superheat is four times as much, or 0.6 K. The inner wires are therefore only 1.88 K hotter than the fluid, a permissible value. However the major benefit over the previous case (Figure D3) comes from the wire spacing going to zero, an unachievable ideal limit. To find how closely the limit can be approached in practice would require fabrication trials.

As a last case to show feasibility of removing the AC losses, consider gaseous helium as the coolant. If liquid hydrogen fuel is not used on the aircraft, then the refrigeration required for the superconducting machines would be provided by cryocoolers. The coolant circulated from cryocoolers to superconducting machines would likely be helium gas under pressure. It is expected that the gaseous coolant will require higher pumping power to achieve the same degree of heat removal. We will try to estimate whether that is prohibitive for the level of AC loss in our standard case.

By using equations presented in Appendix C, we find that the heat transfer coefficient mentioned in connection with the Figure 14 system of 6,955 W/(K·m^2) could be matched in gaseous He at a pressure of 60 psi if the mass flow rate in each channel is 0.17 g/s. The superconducting wire temperatures would then be the same as in the liquid hydrogen cooled case of Figure 14, with a superheat of 0.15 K above the coolant temperature. The pressure drop required to force that value of mass flow is calculated to be 9.8 psi, a seemingly nonprohibitive value. However, the work needed to force the flow through the cooling channel is unfortunately 1.45 W, which is nearly 6 times the 0.25 W of AC loss absorbed in the channel. This additional inefficiency is unacceptable.

However, if we reduce the flow rate, we can sacrifice heat transfer coefficient in favor of lower pumping power, up until the wire superheat becomes a problem. For 60 psi pressure and a flow rate of 0.09 g/s per channel, the heat transfer coefficient drops to 4,218 W/(K·m^2), which increases the wire superheat only to 0.25 K, a reasonable value. The pumping power drops to 0.25 W per channel, the same as the AC loss. The fluid pumping power would be doubling the inefficiency.

A still further reduction in helium flow rate can get the pumping power to be a small fraction of the AC loss. Maintaining the 60 psi pressure, but reducing the mass flow rate to 0.03 g/s per channel, yields a heat transfer coefficient of 1,751 W/(K·m^2) and a consequent superheat of 0.6 K at a pumping power of 0.012 W per channel. This pumping power is only 5 percent of the AC loss.

In summary, up to four-layer epoxied coils may be feasible with liquid hydrogen or gaseous helium as a coolant, especially if the thermal conductivity of the epoxy can be improved with fillers.

Appendix E.—Eddy Current Loss in Round Copper Wire at 20 K

To calculate the eddy current loss in a round wire in a transverse magnetic field, we follow Ferreira (1994) Equations (A7) and (A8). The eddy current loss in commercial copper wire of typical dimensions used at room temperature can be very large at low temperatures where the resistivity approaches 1 percent of its room temperature value.

First, we need to calculate the skin depth δ for the relevant frequency:

$$\delta = \left[\frac{2\rho}{\omega \mu_o} \right]^{1/2}$$

where $\omega = 2\pi f$, f is the frequency, μ_o is the permeability of free space, and ρ is the resistivity of the metal.

Then the loss per unit length of wire P from Ferreira Equations (A7) and (A8) is

$$P = 2\pi\gamma\rho H^2 \left\{ \frac{\left[ber_2(\gamma) ber'(\gamma) + bei_2(\gamma) ber'(\gamma) \right]}{ber^2(\gamma) + bei^2(\gamma)} \right\} \tag{E1}$$

where H is the amplitude of the applied field, $\gamma = d \Big/ \left(\delta\sqrt{2} \right)$ and d is the wire diameter.

For low frequencies f and small wire, Equation (E1) reduces to the following simple formula for the loss per unit length:

$$P = \frac{\pi^3 \mu_o^2}{32\rho} f^2 d^4 H^2$$

Appendix F.—Magnetoresistance of Copper at 20 K

The resistivity of metals is generally increased by the application of a magnetic field perpendicular to the direction of current flow. At normal temperatures, the increase is rarely noticeable, but in pure metals at low temperatures, the increase can be substantial. For copper, the fractional increase in resistance can be conveniently shown on a Kohler plot (Figure F1) of that increase versus the magnetic field H multiplied by the ratio of room temperature resistivity to the resistivity at the temperature of interest.

From the Kohler plot from Fickett (1971), see that for copper with residual resistive ratio of 100, magnetoresistance adds about 12 percent to the resistance.

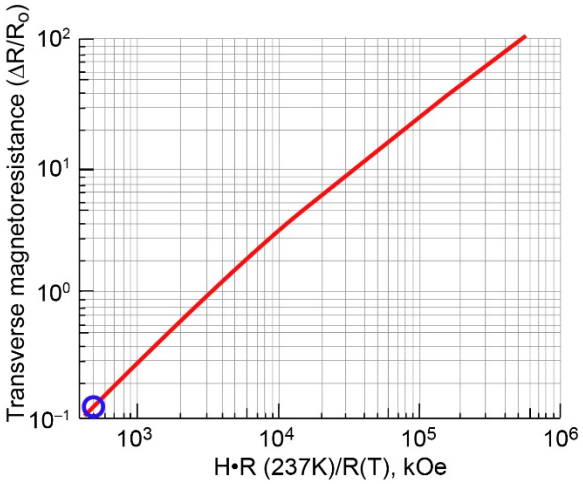

Figure F1.—Kohler plot for polycrystalline copper wire. Note that abscissa is in kilooersted.

References

Bean, C.P. (1962): Magnetization of Hard Superconductors. Phys. Rev. Lett., vol. 8, pp. 250–253.

Brown, Gerald V. (2011): Weights and Efficiencies of Electric Components of a Turboelectric Aircraft Propulsion System. AIAA 2011–225.

Carr, W.J., Jr.; and Wagner, G.R. (1986): Surface Current and Hysteresis in Fine Filament NbTi Superconductors. J. Appl. Phys., vol. 60, no. 1, pp. 342–345.

Carr, W.J., Jr. (2001): AC Loss and Macroscopic Theory of Superconductors. Second ed., Taylor & Francis, New York, NY.

Chen, Peng, et al.: Development of a Persistent Superconducting Joint Between Bi-2212/Ag-Alloy Multifilamentary Round Wires. Supercond. Sci. Tech., vol. 30, no. 2, PMID 025020, 2017.

Felder, James L.; Kim, Hyun Dae; and Brown, Gerald V. (2009): Turboelectric Distributed Propulsion Engine Cycle Analysis for Hybrid-Wing-Body Aircraft. AIAA 2009–1132.

Ferreira, Jan A. (1994): Improved Analytical Modeling of Conductive Losses in Magnetic Components. IEEE Trans. Power Electron., vol. 9, no. 1, pp. 127–131.

Fickett, F.R. (1971): Magnetoresistance of Very Pure Polycrystalline Aluminum. Phys. Rev. B, vol. 3, no. 6.

Incropera, Frank P., et al. (2007): Fundamentals of Heat and Mass Transfer. Sixth ed., John Wiley & Sons, New York, NY, p. 514.

Jansen, Ralph H., et al. (2015): Turboelectric Aircraft Drive Key Performance Parameters and Functional Requirements. AIAA 2015–3890 (NASA/TM—2016-218919). http://ntrs.nasa.gov

Kim, Y.B.; Hempstead, C.F.; and Strnad, A.R. (1963): Magnetization and Critical Supercurrents. Phys. Rev., vol. 129, no. 2.

Larbalestier, David (2016): Superconductors for the Future—From the Perspective of the Past. Plenary Presentation 1PL–01 given at the Applied Superconductivity Conference, Denver, CO.

Lee, Jiho; and Ko, Tae Kuk (2014): Estimation of the Engineering Critical Current Criteria for HTS Wire Carrying an Alternating Current. IEEE Trans. Appl. Supercond., vol. 24, no. 3.

Lorin, Clement; and Masson, Philippe J. (2013): Numerical Analysis of the Impact of Elliptical Fields on Magnetization Losses. IEEE Trans. Appl. Supercond., vol. 23, no. 3.

Meyerhoff, R.W. (1995): Development of a Rigid AC Superconducting Power Transmission Line. Advances in Cryogenic Engineering, K.D. Timmerhaus, ed., Vol. 19, Springer, New York, NY, pp. 101–108.

Solid Material Solutions, LLC (2019): Bi2212 Superconductors for High-Power Density Motors for Aero Propulsion. Phase I SBIR Report, Contract Number 80NSSC18P1899.

Sumption, M.D., et al. (2016): AC Loss Measurements of MgB_2 Strands Designed for Motor and Generator Applications. Applied Superconductivity Conference 2016, Denver, CO.

Tomsic, Michael J., et al. (2015): Development of MgB_2 Superconductors and Coils for Practical Applications. Presented at the Cryogenic Engineering Conference/International Cryogenic Materials Conference, Tucson, AZ.